J Med Syst (2016) 40: 166
DOI 10.1007/s10916-016-0523-4

Neonatal Jaundice Detection System

Mustafa Aydın[1] · **Fırat Hardalaç**[2] · **Berkan Ural**[2] · **Serhat Karap**[2]

Received: 26 January 2016 / Accepted: 9 May 2016 / Published online: 26 May 2016

Abstract Neonatal jaundice is a common condition that occurs in newborn infants in the first week of life. Today, techniques used for detection are required blood samples and other clinical testing with special equipment. The aim of this study is creating a non-invasive system to control and to detect the jaundice periodically and helping doctors for early diagnosis. In this work, first, a patient group which is consisted from jaundiced babies and a control group which is consisted from healthy babies are prepared, then between 24 and 48 h after birth, 40 jaundiced and 40 healthy newborns are chosen. Second, advanced image processing techniques are used on the images which are taken with a standard smartphone and the color calibration card. Segmentation, pixel similarity and white balancing methods are used as image processing techniques and RGB values and pixels' important information are obtained exactly. Third, during feature extraction stage, with using colormap transformations and feature calculation, comparisons are done in RGB plane between color change values and the 8-color calibration card which is specially designed. Finally, in the bilirubin level estimation stage, kNN and SVR machine learning regressions are used on the dataset which are obtained from feature extraction. At the end of the process, when the control group is based on for comparisons, jaundice is succesfully detected for 40 jaundiced infants and the success rate is 85 %. Obtained bilirubin estimation results are consisted with bilirubin results which are obtained from the standard blood test and the compliance rate is 85 %.

Keywords Neonatal jaundice · Bilirubin · Image processing · Image segmentation · Machine learning regressions

This article is part of the Topical Collection on *Transactional Processing Systems*

✉ Fırat Hardalaç
hardalac@gmail.com

[1] Pediatrics-Neonatology, Fırat University, Elazig, Turkey

[2] Electrical Electronics Engineering, Gazi University, Ankara, Turkey

Introduction

Neonatal jaundice or neonatal icterus is a disease which has been known since ancient times and today, diagnostic and therapeutic methods are constantly being developed [1]. The first information about neonatal jaundice was written in the book of "Ein Regiment der Kinder" by Metlinger in 1473 [2].

Neonatal jaundice or neonatal hyperbilirubinemia is clearly seen when bilirubin level exceeds 5 mg/dl (85 mmol/l) in infants' blood [3]. In the first week of life, bilirubin level rises in every newborn infants. According to the worldwide standards, jaundice is detected in almost 60 % of the healthy full-term babies and 80 % of the preterm babies [4].

During the fetal period, red blood cells in the baby's blood are quite different than a normal human's red blood cells. This red blood cells contain "fetal hemoglobin (HbF)" [5]. The most important feature of these red blood cells is rapidly disintegrating after birth. In the body, because of this occasion, new red blood cells which contain a new kind of hemoglobin "adult hemoglobin (HbA)" are created simultaneously [6]. In newborn infants, two factors are responsible from development of jaundice - the breakdown of HbF as it is replaced with HbA, and the relatively immature metabolic pathways of the liver, which are unable to conjugate and so excrete bilirubin as quickly as an adult [7]. Generally, bilirubin is processed in the liver in the body and more of them is converted and sent to the rectum [8]. When more of the bilirubin can not be processed by baby's liver, this bilirubin is become to accumulate in

baby's blood, which called as hyperbilirubinemia. Bilirubin is a yellow color pigment and, therefore, when excess of the bilirubin is accumulated in the skin, symptoms of jaundice occurs [9].

Neonatal jaundice is a clinical condition which may resolve without any intervention in the majority of babies; however, it is highly important that this critical period should be passed under a doctor's supervision [10]. Otherwise, when the serum bilirubin level exceeds the critical level; permanent brain damage due to accumulation of the bilirubin in the brain, a disease called kernicterus, can clearly be seen [11, 12].

Severe neonatal jaundice is a pediatric emergency because it may cause to kernicterus which can result in chronic handicapping conditions like sensorineural deafness or cerebral palsy in those who survive. The goal of the management of severe neonatal jaundice is therefore to rapidly reduce the serum bilirubin level to prevent kernicterus. There are a variety of treatment methods about neonatal jaundice; which are still being developed. Specific treatment is not necessary for the low level of bilirubin in physiological jaundice; but phototherapy is started if the total bilirubin level exceeds a reliable point, usually by >15 mg/dl, with respect to the postnatal age and weight of the patient, [13]. By using the phototheraphy method, bilirubin is excreted from the body by urine through the kidneys after converted to the water-soluable products [14]. Another important treatment method of severe neonatal hyperbilirubinemia is the exchange transfusion [15]. For this procedure, when serum bilirubin level exceeds the critical levels, usually by >20–25 mg/dl, with respect to the clinical condition and postnatal age and weight of the patient, the only way is an exchange transfusion [16].

In this work, creating a novel and a non-invasive system for detecting jaundice in newborns optimally was generally aimed. First, the 8-color calibration card was used for eliminating the enviromental lightning problems and doing the necessary comparisons with a high performance for the other stages. This card was placed on the baby's abdomen and pictures of the baby were taken with a standard smartphone camera in the proper position and these data were transferred to MATLAB® environment to be processed. Second, obtained images were analyzed with the color based image processing techniques to detect the optimal color tone with using the baby's important body parts, then with using morphological techniques, edits and improvements have been made. After this step, data analysis and calculation were done by machine learning regressions. The last step of the system is to determine and to estimate the optimal bilirubin level in the baby' blood. In the experimental part of the work, a patient group which was consisted from jaundiced babies and a control group which was consisted from healty babies were prepared, then between 24 and 48 h after birth, 40 jaundiced and 40 healthy newborns were chosen for these groups and analysis and comparisons were generally done for 80 infants. Finally, when the control group was based on, for 40 jaundiced newborns, jaundice was detected successfully and the success rate was 85 %. Obtained bilirubin estimation results were consisted with bilirubin results which were obtained from the standard blood test and the compliance rate was 85 %.

In literature, there were limited studies about jaundice detection for neonatals and there was not any adequate resources about these works. So, more comments could not be made about their performance and achievements. Apart from this study, there have been no works that contained advanced image processing algorithms and machine learning regressions yet. In the Results and Discussion part, comparisons and performance analysis were clearly done between the neonatal jaundice system and some works that were related to the general jaundice. The statistical test results were obtained from these limited works and neonatal jaundice system's statistical results were compared with the other works' results in this part in detail.

Materials and methods

Data collection phase

Methods that were used in this study were applied to 40 healthy and 40 jaundiced babies' images. For this work, the necessary document of the ethical rules was taken by Fırat Hardalaç in Ankara, Turkey. Indeed, these data were collected from Fırat University Faculty of Medicine Neonatal Department with the cooperation of Assoc. Prof. Mustafa Aydın. Test subjects' age (hour), bilirubin level (mg/dl) and hemolysis (n,%) average values were 33 h, 11.9 mg/dl and 15 %, respectively. Figure 1 illustrated the

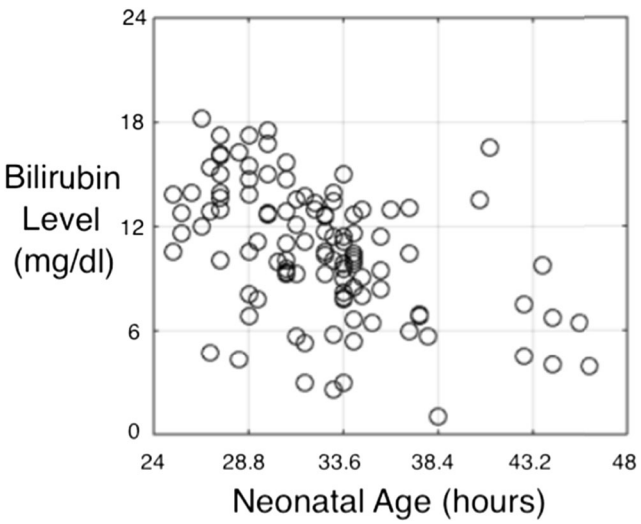

Fig. 1 The distribution of bilirubin levels versus age value (hours) for 40 jaundiced babies

distribution of bilirubin levels versus age value (hours) for 40 jaundiced babies.

During the data entry phase, while baby was in the recumbent position, the 8-color calibration card was placed on the baby's abdominal region. With using 12 MP Samsung Galaxy Alpha smartphone and when using this smartphone camera with no flash, baby's whole body photos were taken and results were obtained. The resolution value of the obtained images was 96 dpi and for the other stage, these images were transferred to MATLAB® environment and image processing methods and machine learning regressions were used on these images, respectively.

Structure of the system

The flowchart of the system was generally given in Fig. 2 and every step of the process was mentioned below in detail.

The type and the size of the image data were uint8 and 440 um × 440 um, respectively. The first stage of the system was called as color based balancing. At this stage, segmentation process was performed on the images. With using segmentation, important regions and their information were preserved and also unused regions were rearranged in the black color tone [17]. Second, with using pixel similarity method, some of the missing colors on the color calibration card is provided to be brought back [18]. Third, with using white balancing method, images were being independent from ambient light, reflections and shadows [19]. The second stage of the system was called feature extraction. At this stage, the information data about baby's skin and the colors of the color calibration card were obtained in RGB, YCbCr and Lab color spaces with using colormap transformations and feature calculation [20]. The third stage of the system was called machine learning regressions. At this stage, kNN (k-Nearest Neighbor) and SVR (Support Vector Regression) algorithms were used on the dataset which were obtained from the second stage. The fourth stage of the system was bilirubin level estimation. At this stage, bilirubin level estimation process was achieved with using obtained regression results [21]. The details of the processes were described below in detail.

Color based balancing

Image segmentation Segmentation was the first step of the system. Image segmentation was described as seperating the image in each of the regions where different properties were kept. Color calibration card which was used in this work was specially designed and to obtain this card an advanced laser printer and an uncoated paper were used. The example of the color calibration card was given in Fig. 3 [21].

With using the color calibration card that was given in Fig. 3, segmentation process was performed on the babies' images (Fig. 4) [21]. During segmentation, each color on the calibration card was evaluated seperately and estimation process was achieved. The color calibration card made the baby independent from external stimuli and after using the card, the image was ready for processing [21]. The captured image was subjected to the segmentation process. First, for this process, the captured image was divided into the desired segments, then 8 main colors and jaundiced regions' colors were compared [22]. Second, jaundiced regions were concretized via segmentation and other regions were eliminated. For segmentation process, point-based and region-based detection techniques were used, respectively [23].

After this step, third, the image was filtered through the Gauss filter. After this situation, environmental noises and blurring were eliminated [24].

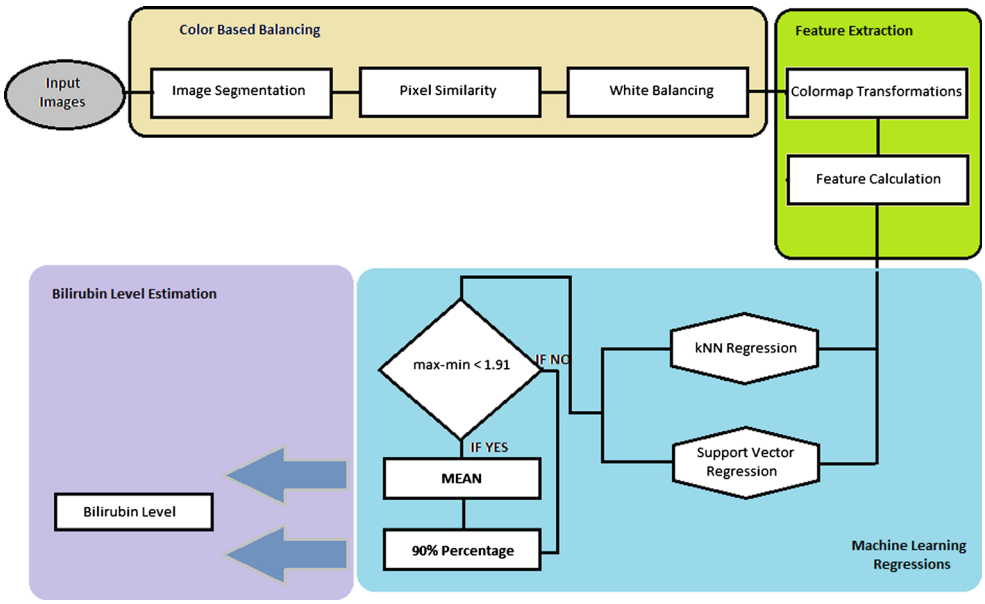

Fig. 2 Flowchart of the neonatal jaundice detection system

Fig. 3 Color calibration card example [21]

After the noise reduction process by filtering, thresholding was performed on the image and some regions which belonged to the baby and color calibration card were seperated from the image. In this phase, regions that were not adjacent to the baby and color calibration card were represented in black color tone in the image. For insufficient cases to determine the threshold value, more specific local transformations were used for segmentation [25]. When analyzing the color callibration card's colors in RGB plane, vertical and horizontal edge detection algorithms were used [26].

Pixel similarity The regions that belonged to the baby and the card were obtained after segmentation, also other areas were rearranged in black color tone. But, after segmentation, some colors lost and this occasion was clearly seen on the color calibration card. In this phase, with using pixel similarity method, missing colors were brought back on the color calibration card [27]. During this process, when one center pixel is based on, the distance between this pixel and other neighbors were calculated and obtained results were collected in a matrix. Then, the obtained matrix represented a new RGB image [28]. In the new image, all missing colors were brought back on the color calibration card and P_1 ve P_2 pixels' neighborly relations were calculated with using the Eqs. (1) and (2), respectively.

$$\mu(P_1, P_2) = \exp\left(-(\|P_1–P_2\|/D_n)^2\right) \quad (1)$$

$$\|P_1–P_2\| = \frac{1}{\sqrt{3}}\left[(R_1–R_2)^2 + (G_1–G_2)^2 + (B_1–B_2)^2\right]^{1/2} \quad (2)$$

White balancing One of the important problems of the image processing is that different results can be obtained for an image because of environmental and lightning differences [29]. This occasion is usually undesirable. For an image, the same results can be expected to be obtained from different light intensities and this is generally desirable [30].

The aim of white balancing is to make the original image independent from the luminous intensity [31]. According to the luminous intensity and the location of the resource, some differences can be obtained from the process of determining the skin color. To eliminate this problem, normalized red, green and blue values were calculated. Normalization calculation was achieved when each of the color was divided into the total value [32].

Feature extraction

Colormap transformations In this step, yellow areas which belonged to the baby's important parts of the body were detected. So, first, images were converted from RGB to YCbCr and Lab color spaces [33]. In addition, with using feature extraction, the reduction process in image size was performed [34]. At the end, the reduced image was obtained for other stages. With using the colormap transformations, all colors of the color calibration card and baby's skin color were compared in RGB color space.

Feature calculation In this step, the average values of the images which were processed in YCbCr and Lab color spaces were calculated for each color channel and at the end of the calculation, totally 9 features were obtained from this step.

Alongside color transformation, with using a linear color gradient, the color difference value was calculated. Gradient calculation was altered with the 3 × 3 Sobel filter and this filter was applied to the each channel of RGB. At the end of the step, totally 3 features were obtained.

As a result of the feature calculation step, totally 12 features were obtained and these features were taken to be trained via machine learning algorithms.

Machine learning regressions

For this step, kNN (k-Nearest Neighbor) and SVR (Support Vector Regression) regressions were chosen to use because

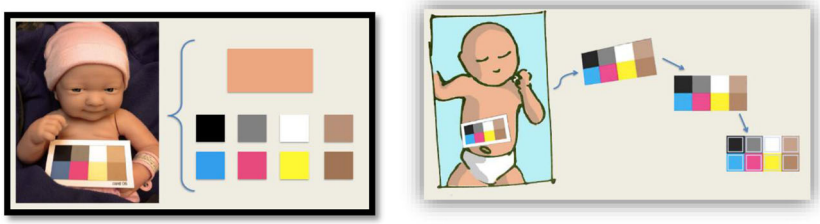

Fig. 4 The process of segmentation by using the color calibration card [21]

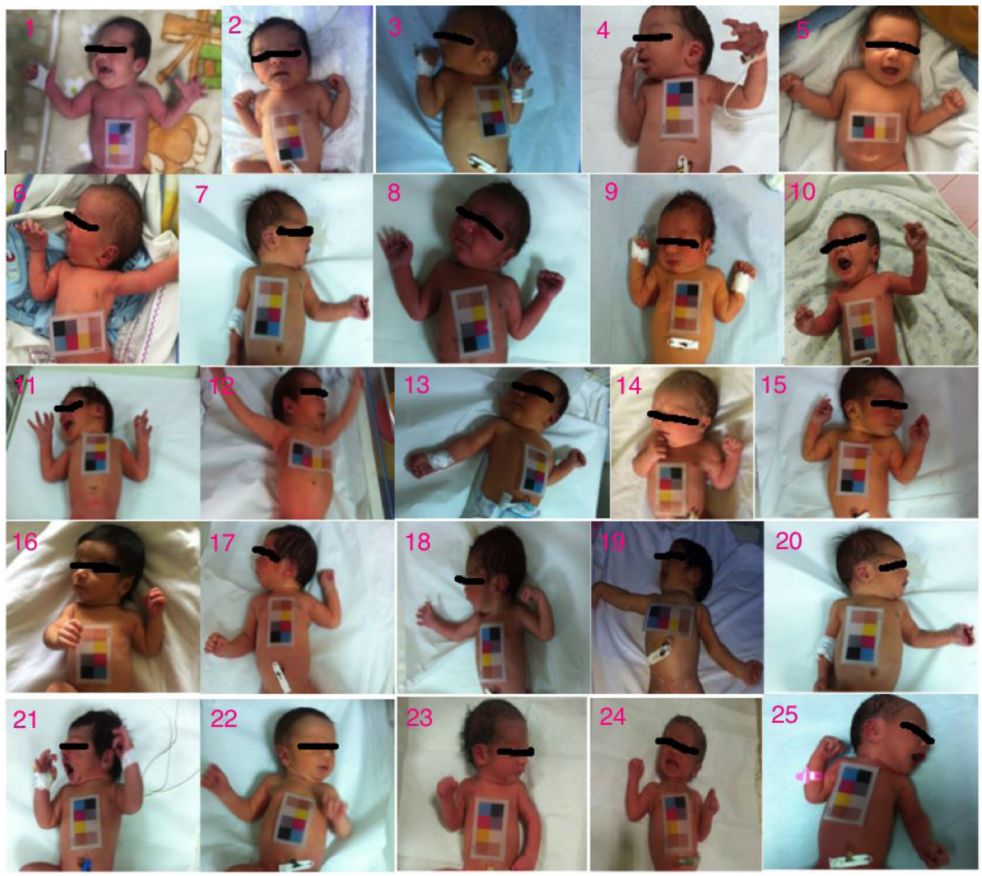

Fig. 5 Input images of the system

these algorithms were successful for this system. Each of the regression technique can compare the feature data in a different angle. First, 2 different regression algorithms were used on the dataset. Second, the output of each regression which was based on a fixed threshold was evaluated and bilirubin estimation process was performed using the threshold value and dataset. Below, kNN (k-Nearest Neighbor) and SVR (Support Vector Regression) were explained in detail.

kNN (k-Nearest Neighbor) The first algorithm was kNN (k-Nearest Neighbor) and for this algorithm, the coefficient was chosen as k = 5. This regression algorithm was quite succesfull to determine the bilirubin level locally [35]. Bilirubin values and specific feature data were in this regression. When a nondefined test vector was analyzed, k-neareast neighbors were found around the test vector in the feature dataset [36].

SVR (Support Vector Regressions) The first resgession which was used was generally linear, but SVR algorithm was non-linear [37]. When determining the relationships between linear relationships, generally, Support Vector Regressions were used. The aim of the regression was finding a linear regression function in a high dimensional feature space [38]. Then, input data was mapped to the space with using the potential non-linear function [39]. For this step, totally 2 SVRs were adapted for training, these were kernel and non-linear sigmoid basis functions.

Bilirubin level estimation

In the bilirubin level estimation step, the threshold value was chosen after multiple trials. Then, this value was chosen as 1.91. For this step, first, maximum and minimum output value were based on to use. Then, when the difference between these values was less than the threshold value, the average of the maximum and minimum values was calculated and the output result was the system's final bilirubin level estimation value [21]. Otherwise, 90 % of the difference of maximum and minimum values was calculated and obtained result was the system's final bilirubin level estimation [21].

Results and discussion

The first step of the system was defining input data with images. Some of the input images which was loaded to the

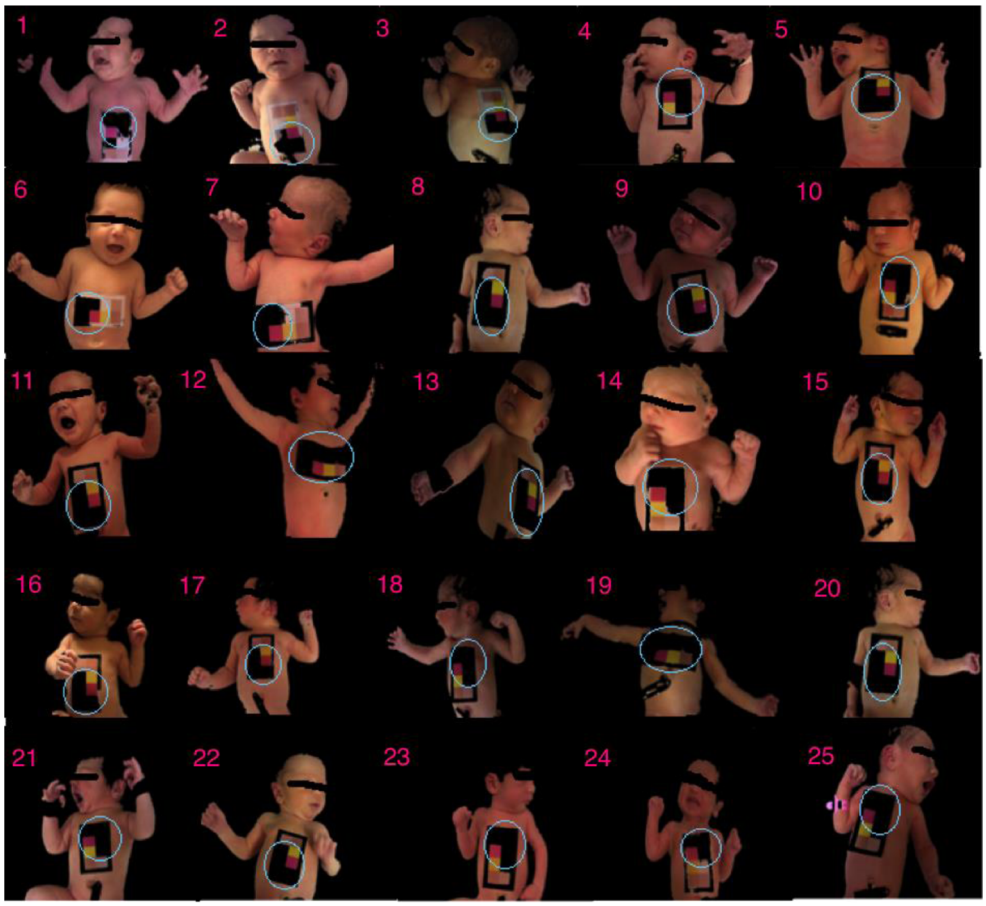

Fig. 6 Image segmentation results

system were clearly shown in Fig. 5. In addition, in Fig. 5, each of the babies was numerized respectively, so analysis and comparisons were achieved easily.

The first stage of the system was color based balancing. The first step of the color based balancing was image segmentation. With using segmentation, unused parts of the images were subtracted from the images and only important areas were remained back. Segmentation results were represented in Fig. 6.

When segmentation results which were given above were analyzed in detail, some colors lost on the color calibration card for each image. For example, when the results of baby-4 and baby-22 were investigated, it was seen that segmentation was achieved successfully and the success rate was calculated as 100 %. Indeed, after segmentation process, 4 main colors lost on the color calibration card and these areas were rearaanged in black color tone. The reason for this occasion was based on the neigborly relations of the pixels in the images, so pixels of the missing color tones which were not located around their neighbors were represented in black color tone in the final statement.

When this step was analyzed for 80 images, during the segmentation process, the success rate was calculated as 100 % and the process time was obtained as 1.8 s and maximum performance and success was obtained from the system. Finally, with using segmentation, areas which were related to the baby's body were remained and other areas of the image were represented in black color tone.

The second step of the color based balancing was pixel similarity method. In this step, with using pixel similarity method, missing colors were brought back on the color calibration card. For this step, each of the images was numerized and obtained output images were given in Fig. 7 in detail.

When the images which were given above were analyzed, with using pixel similarity method, missing colors were brought back on the color calibration card for each of the images. For example, when the results of baby 4 and baby 22 were investigated, the missing colors were brought back successfully for these images and the success rate was calculated as 100 %. At the end of this process, for each of 80 images, the success rate was calculated as 100 % and the process time was obtained as 1,3 s.

The third step of the color based balancing was white balancing. In this step, the conditions of increasing resolution and sharpness on the images were generally studied. Resulted images obtained from this step were given in Fig. 8.

The purpose of the white balancing was to make the image independent from ambient lightning, reflections and shadows.

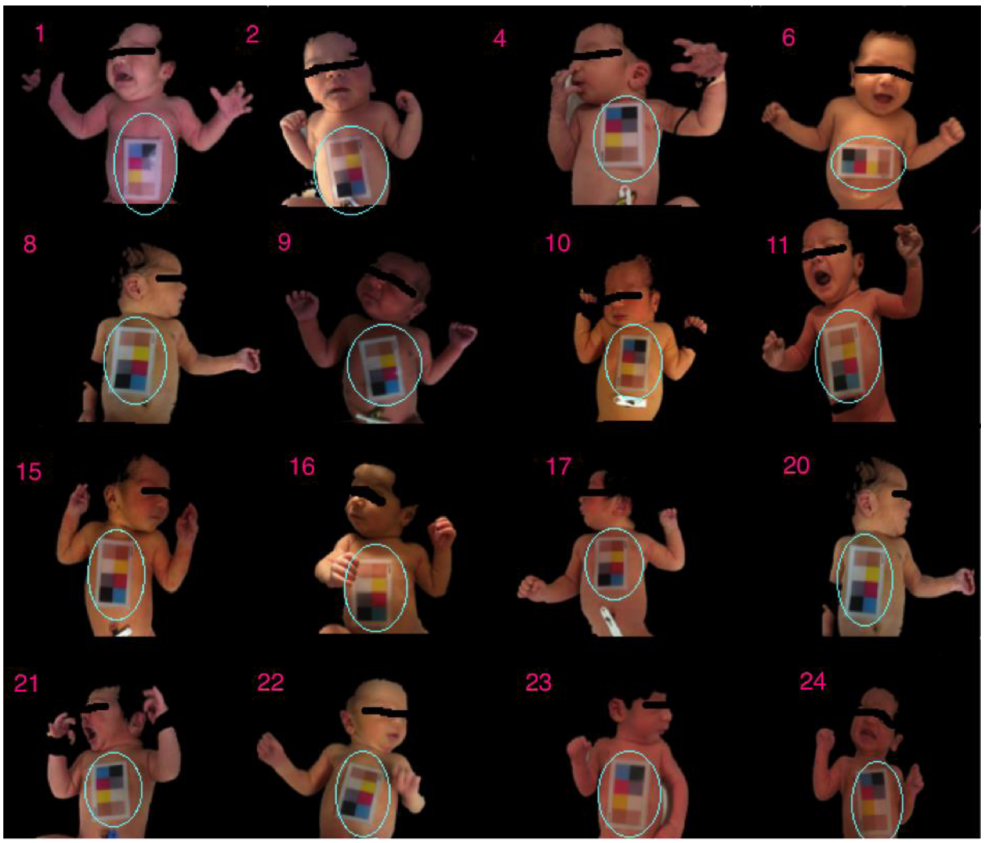

Fig. 7 Results of pixel similarity method application

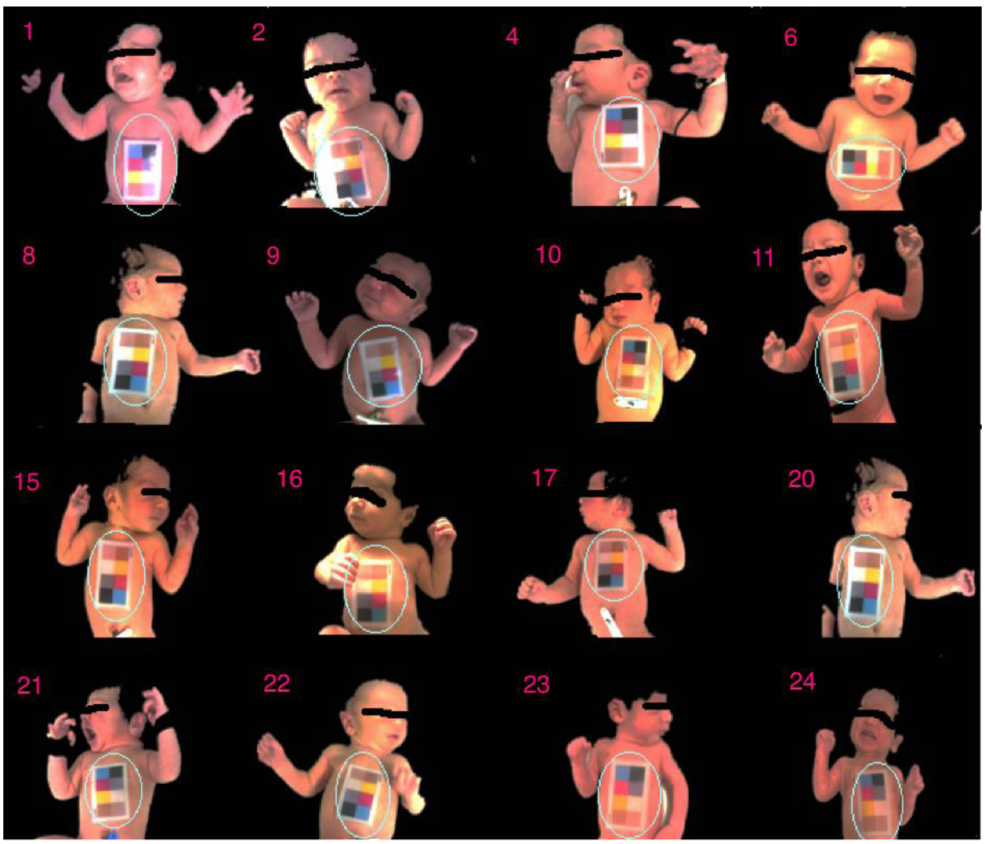

Fig. 8 Results of white balancing application

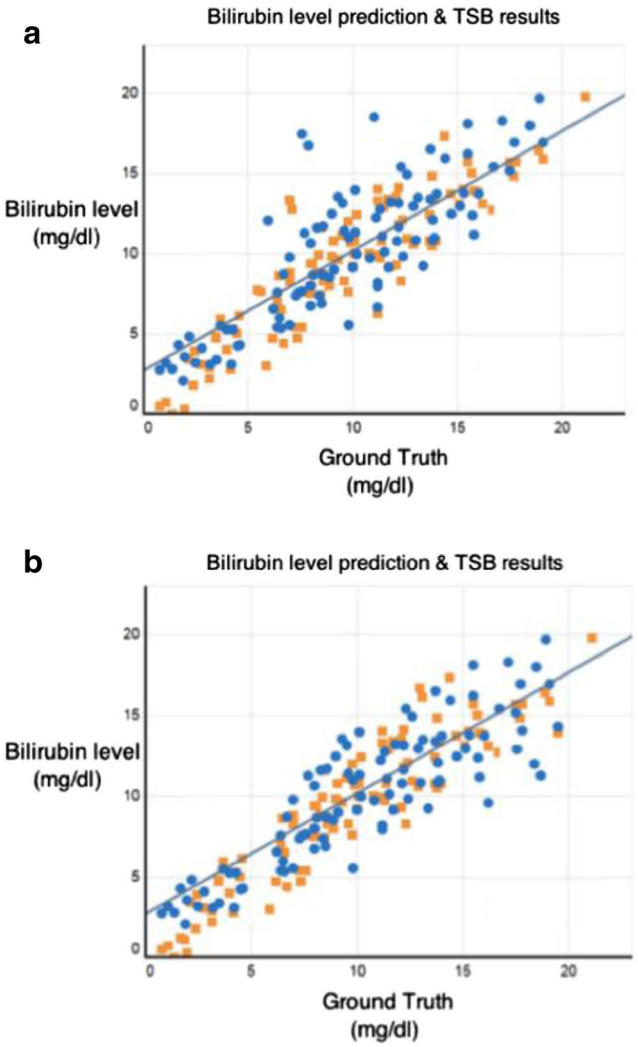

Fig. 9 The distribution of the system's estimation results and general bilirubin results (TSB) which were obtained from standard blood test around the decision boundary. (for this distribution, *blue circles* represented our system's bilirubin estimation values, *orange squares* represents general bilirubin results (TSB) which were obtained from standard blood test); (**a**) The distribution of the data around the decision boundary with using SVR algorithm, (**b**) The distribution of the data around the decision boundary with using kNN algorithm

In this step, resulted images were analyzed and for example, when images of baby 4 and baby 22 were analyzed in detail, at the end of the white balancing method, the rate of the resolution value of the pixels was increased from 92 to 100 and clarity and sharpness were gained to the images. When this step was analyzed for 80 baby images, the success rate of the white balancing was calculated as 100 % and the process time was obtained as 2,1 s. Indeed, it was clearly seen that final images were become independent from ambient lightning, reflections and shadows.

The second stage of the system was feature extraction. In this stage, with using colormap transformations and feature calculation, for each of the images, the information of the every pixel in RGB, YCrCb and Lab color spaces were transferred to the R, G, B; Y, Cr, Cb; L, a, b color channels and then, machine learning regressions were performed on the color channels' dataset in MATLAB® environment.

Totally, for 9 channels and 80 images, dataset value was calculated as 440*440*9 = 1.742.400. But, in each image, when black areas were defined as unnecessary areas, new dataset value was calculated as 900.000. In addition, with using a linear color gradient, color difference on the color calibration card in RGB color space was calculated and for R, G, B channels, this value was obtained as 110*180*3 = 59.400. Finally, obtained feature value obtained as 959.400 was processed with using kNN (k-nearest neighbor) and SVR (Support Vector Regression) machine learning regressions. For this step, first, maximum and minimum output value were based on to use. Then, when the difference between these values was less than the threshold value, the average of the maximum and minimum values was calculated and the output result was the system's final bilirubin level estimation value. Otherwise, 90 % of the difference of maximum and minimum values was calculated and obtained result was the system's final bilirubin level estimation.

The third stage of the system was machine learning regressions and kNN and SVR algorithms were performed on the dataset. The outputs of this process were sent to the bilirubin level estimation step. In this step, algorithms were used on each of the feature information and totally 959.400 new feature results were obtained. At the end of the machine learning process, maximum and minimum values were obtained in detail. In bilirubin level estimation step, when the difference between maximum and minimum values was based on to use, the bilirubin level estimation decision loop was carried out. In this step, threshold value was chosen as 1,91 after multiple trials. For this step, first, maximum and minimum output value were based on to use. Then, when the difference between these values was less than the threshold value, the average of the maximum and minimum values was calculated and the output result was the system's final bilirubin level estimation value. Otherwise, 90 % of the difference of maximum and minimum values was calculated and obtained result was the system's final bilirubin

Table 1 F-statistical test results

Predicted Bilirubin Level	Region of Interest	Did RGB values normalize?	Statistical F-test result
$y_{skin,\ normalized}$	Skin	Yes	0.80 ($p > 0.06$)
y_{skin}	Skin	No	0.85 ($p > 0.06$)

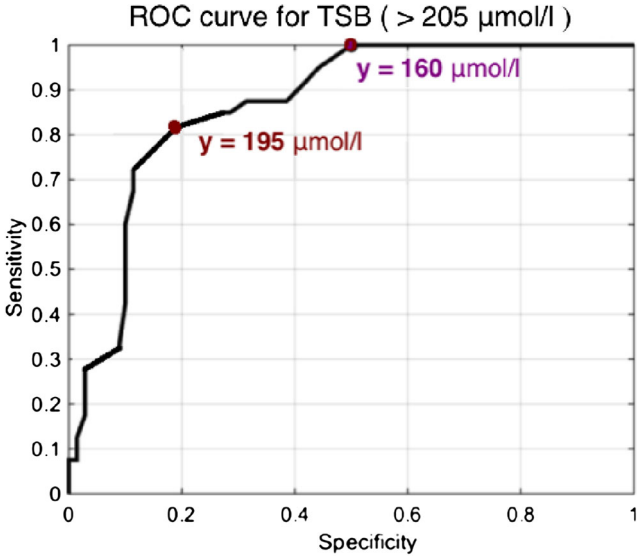

Fig. 10 ROC curve for neonatal jaundice detection system

level estimation. Finally, the distribution of the estimation data which was around the decision boundary was given graphically in Fig. 9.

The distribution graphics were obtained specifically with using SVR and kNN algorithms and when a decision boundary was created, bilirubin estimation results which were obtained from our system non-invasively were compared to the bilirubin estimation results which were obtained from the standard blood test invasively. When specifically designed graphics were analyzed in detail, estimation results which converged to the decision boundary were considered as true values. According to the obtained data, when linear correlation value was equal to 0.81, for 40 jaundiced infants, bilirubin estimation results obtained from our system were consistent with bilirubin estimation results obtained from standard blood test and the compliance rate was 85 %. Also, for easy comparisons, kNN and SVR algorithms were classified and analyzed in each other respectively. With using kNN algorithm, more accurate results were obtained than SVR algorithm and the compliance rate between our system's results and standart blood test results was 85 %. For SVR algorithm, the compliance rate between our system's results and standart blood test results was 75 %. Finally, as a comment, maximum success and performance were obtained from our system when kNN algorithm was used and obtained results were highly consistent with the standard blood test results.

Statistical analysis

Bilirubin level data which were obtained from neonatal jaundice detection system were adapted to the F-statistical test to evaluate the accuracy of the dataset and performance of the system. In this step, a comparing process was performed between the system's bilirubin level estimation results and the standard blood test results and the similarity rate of the two different results was clearly investigated. According to the results, when the significance case was $p > 0.06$, a correlation was found between neonatal jaundice detection system's bilirubin results and standard blood test results. The compliance rate between these values was calculated as 85 % according to the F-statistical test. Obtained results were represented in Table 1 in detail.

Moreover, to determine the accuracy rate of the bilirubin levels and to calculate the system's performance were achieved in the other step and ROC (Receiving Operating Characteristics) analysis was used to analyze the dataset in detail. When preparing the ROC curve, measured data which was obtained from blood test was based on to use. During this process, threshold value (y_{sc}) was chosen as 205 µmol/l. If obtained value was higher than the defined threshold value, a greater true positive rate (TPR) value and false positive rate (FPR) value could be obtained. When the threshold level incresed, a fluctuation occured in TPR and FPR values. Finally, ROC curve for this situation was shown in Fig. 10.

When ROC curve which was given above was analyzed, threshold value was chosen as 205 µmol/l. Cut-off threshold value (y) was calculated optimally with F-statistical test and the equation for calculation was given in (3) below.

$$J = \text{sensitivitiy} + \text{specificity} - 1 = \text{TPR} - \text{FPR} \quad (3)$$

The first y point was varied between a higher TPR value and a lower FPR value. When sensitivity value was 0.83 and

Table 2 Results of different works and neonatal jaundice detection system

Work	Method	Body Part	Linear Correlation, r (n)	Bland-Altman test: mean difference - standart deviation (µmol/l)
Leartveravat, S., 2009 [40]	Digital photography	Sternum	0.86 (n = 61)	N/A
Goel, M. , 2014 [21]	Digital photography	Sternum & Forehead	0.84 (n = 100)	N/A
Vandermeer, B. 2013 [41]	BiliCheck, JM-102/103	Forehead, Sternum	0.83 (n = 16), 0.83 (n = 10)	0.06 ± 29.46(n = 912), 3.80 ± 24.06 (n = 265)
Ural, B., 2015 (this study)	Digital photography	Skin (Normalized), Skin	0.80 (n = 80), 0.85 (n = 40)	0.01 ± 38.61, 0.011 ± 38.40

specificity value was 0.195, y value was calculated as 195 μmol/l. In addition, one more specific point was analyzed and when sensitivity value was 1 and specificity value was 0.50, y value was calculated as 160 μmol/l. Finally, 100 % success rate and approximately 1.95 s process time of neonatal jaundice detection system were supported with ROC curve and analysis.

The final step was making comparisons and performance analysis between our unique neonatal jaundice detection system and different works that were contained different methods about jaundice. Comparison results were classified and given in Table 2 in detail, respectively.

In Table 2, generally, the results of different works and methods that were about jaundice and the results of our neonatal jaundice detection system were listed in a table format. First of all, in 2009, S. Leartveravat and friends [40] achieved to detect jaundice with 61 subjects and using digital photography method for sternum. According to the results, a correlation was found between obtained results and this value was calculated as 0.86. Secondly, M. Goel and friends [21] achieved to detect jaundice with 100 participants and using digital photography method for sternum and forehead and at the end, a correlation was found between obtained results and this value was calculated as 0.84. Thirdly, B. Vandermeer and friends [41] achieved to detect jaundice with a limited number of participants and using measurement methods for forehead and sternum and at the end, a correlation was found between obtained results and this value was calculated as 0.83 for each of them. Fourthly, in our neonatal jaundice detection system, we achieved to detect neonatal jaundice in the optimal time for totally 80 test subjects and with using digital photography method babies' skin and the color differences were analyzed. At the end of the process, a correlation was found between obtained results and this value was calculated as 0.85. This system has advanced methods and techniques and also, according to the obtained results, neonatal jaundice was detected optimally with a high performance.

Results

In this study, the aim was creating a non-invasive system to detect and control the jaundice and helping doctors for early diagnosis. Generally, when 40 healthy infants were based on to use, for 40 jaundiced neonatals, the results which were obtained from the flowchart were compared to the standart blood test measurements. Because of the sensitivity of the newborn babies and the courtesy of the vessels, our proposed neonatal jaundice detection system was used commonly to detect the jaundice non-invasively on time and this system gave users accessibility and short processing time for detection. When the processes of the system were investigated, for 40 jaundiced babies, jaundice was detected successfully and optimally in a short time and the success rate of the system was calculated as 85 %. Indeed, this value's accuracy was supported with the F-statistical test and ROC curve and analysis. Then, our system was compared with the other works that were contain jaundice detection and different methods. Finally, it was observed that our system had a unique and novel software, high quality and short processing time. If this study is developed and adapted for the different other diseases, for diagnosing stages, optimal and successful results can be obtained from the system.

References

1. Click, R., Dahl-Smith, J., Fowler, L., DuBose, J., Deneau-Saxton, M., and Herbert, J., An osteopathic approach to reduction of readmissions for neonatal jaundice. *Osteopathic Family Physician.* 5(1):17–23, 2013.
2. Brown A.K., Kernicterus: Past, Present, and Future. NeoReviews. *Am. Acad. Pediatrics*. 4 (2), 2003.
3. Madlon-Kay, D. J., Recognition of the presence and severity of newborn jaundice by parents, nurses, physicians, and icterometer. *Pediatrics*. 100 (3), 1997.
4. Garfunkel, L.C., Kaczorowski, J., Christy, C., Mosby's pediatric clinical advisor: instant diagnosis and treatment. Elsevier Health Sciences. 2002.
5. Arias, I.M., Gartner, L.M., Seifter, S., and Furman, M., Prolonged neonatal unconjugated hyperbilirubinemia associated with breast feeding and a steroid, pregnane-3 (alpha), 20 (beta)-diol in maternal milk that inhibits glucuronide formation in vitro. *J. Clin. Invest.* 43(11):2037–2047, 1964.
6. Murphy, J.F., Hughes, I., Verrier Jones, E.R., Gaskell, S., and Pike, A.W., Pregnanediols and breast-milk jaundice. *Arch. Dis. Child.* 56: 474–476, 1981.
7. Hafkamp, A.M., *Oral treatment of unconjugated hyperbilirubinemia*. Ponsen & Looijen B.V, Wageningen, The Netherlands, 2006.
8. McDonagh, A.F., Movement of bilirubin and bilirubin conjugates across the placenta. *Pediatrics*. 119(5):1032–1033, 2007.
9. Kramer, L.I., Advancement of dermal icterus in the jaundiced newborn. *Amer. J. Dis. Child.* 118:454–458, 1969.
10. Burke, B., Robbins, J., and Hobbs, C., American Academy of Pediatrics Subcommittee on hyperbilirubinemia. Management of hyperbilirubinemia in the newborn infant 35 or more weeks of gestation. *Pediatrics*. 114(1):297–316, 2004.
11. Cremer, R.J., Perryman, P.W., and Richards, D.H., Influence of light on the hyperbilirubinaemia of infants. *The Lancet, Elsevier.* 271(7030):1094–1097, 1958.
12. Cappellini, M.D., Di Montemuros, F.M., Sampietro, M., Tavazzi, D., and Fiorelli, G., The interaction between Gilbert's syndrome and G6PD deficiency influences bilirubin levels. *Br. J. Haematol.* 104(4):928–929, 1999.
13. Newman, T.B., Escobar, G.J., Gonzales, V.M., Armstrong, M.A., Gardner, M.N., Folck, B.F. Frequency of neonatal bilirubin testing and hyperbilirubinemia in a large health maintenance organization. *Pediatrics*. 104 (6), 1999.
14. Stokowski, L.A., Fundamentals of phototherapy for neonatal jaundice. *Adv. Neonatal. Care.* 6(6):303–312, 2006.
15. Geifman-Holtzman, O., Wojtowycz, M., Kosmas, E., and Artal, R., Female Allo-immunization with antibodies known to cause hemolytic disease. *Obstet. Gynecol.* 89(2):272–275, 1997.

16. Mollison, P.L., Engelfriet, C.P., and Contreras, M., *Blood transfusion in clinical medicine*, 10th edn. Blackwell Science, Oxford, 1997.
17. Shapiro, L.G., and Stockman, G.C., *Computer vision*. Prentice-Hall, New Jersey, pp. 279–325, 2001.
18. Rosenfeld, A., and Kak, A.C., *Digital picture processing*. Academic Press, San Diego, 1982.
19. Hsien-Che, L., *Introduction to color imaging science. Cambridge University Press*. pp 450, 2005.
20. Sharma, G., and Bala, R., *Digital color imaging handbook*. CRC Press, Boca Raton, 2002.
21. De Greef, L., Goel, M., Seo, M.J., Larson, E.C., Stout, J.W., Taylor, J.A., Patel, S.N., Bilicam: using mobile phones to monitor newborn jaundice. UbiComp '14 Proceedings of the 2014 ACM International Joint Conference on Pervasive and Ubiquitous Computing. 331–342, 2014.
22. Forcade, N., Le Guyader, C., and Gout, C., Generalized fast marching method: applications to image segmentation. *Numerical Algorithms.* 48(1):189–211, 2008.
23. Horowitz, S.L., Pavlidis, T., Picture segmentation by a directed split and merge procedure. *Proc. ICPR. Denmark*. 424–433, 1974.
24. Haddad, R.A., and Akansu, A.N., A class of fast gaussian binomial filters for speech and image processing. *IEEE Trans. Acoust. Speech Signal Process.* 39(3):723–727, 1991.
25. Haindl, M., Mikes, S., Texture segmentation benchmark. Proc. of the 19th Int. conference on pattern recognition. *IEEE Computer Society.* 1–4, 2008.
26. Chan, T.F., and Vese, L., Active contours without edges. *IEEE Trans. Image Process.* 10(2):266–277, 2001.
27. Pratt, W.K., *Digital image processing*, 4th edn. Hoboken, John Willey & Sons, 2007.
28. Demirci, R., Rule-based automatic segmentation of color images. *AEU Int. J. Electron. Commun.* 60(6):435–442, 2006.
29. Funt, B., Cardei, V., Barnard, K., Learning color constancy. *Proceedings of the Fourth IS&T/SID Color Imaging Conference*, 58–60, 1996.
30. Yule, J.A.C., *Principles of color reproduction*. Wiley, New York, 1967.
31. Viggiano, J.A.S., Comparison of the accuracy of different white balancing options as quantified by their color constancy. Sensors and camera Systems for Scientific, industrial, and digital photography applications V: proceedings of the SPIE. Bellingham. *WA: SPIE: the International Society for Optical Engineering*. 5301: 323–333, 2004.
32. Petschnigg, G., Szeliski, R., Agrawala, M., Cohen, M., Hoppe, H., and Toyama, K., Digital photography with flash and no-flash image pairs. *ACM Trans. Graph.* 23(3):664–672, 2004.
33. Schwarz, M.W., Cowan, W.B., and Beatty, J.C., An experimental comparison of RGB, YIQ, LAB, HSV, and opponent color models. *ACM Trans. Graph.* 6(2):123–158, 1987.
34. Florack, L., and Kuijper, A., The topological structure of scale-space images. *J. Math. Imaging Vision.* 12(1):65–79, 2000.
35. Liu, D.Y., Chen, H.L., Yang, B., Lv, X.E., Li, L.N., and Liu, J., Design of an Enhanced Fuzzy k-nearest neighbor classifier based computer aided diagnostic system for thyroid disease. *J. Med. Syst.* 36(5):3243–3254, 2012.
36. Coomans, D., and Massart, D.L., Alternative k-nearest neighbour rules in supervised pattern recognition: Part 1. k-Nearest neighbour classification by using alternative voting rules. *Anal. Chim. Acta*. 136:15–27, 1982.
37. Nouira, K., and Trabelsi, A., Intelligent monitoring system for intensive care units. *J. Med. Syst.* 36(4):2309–2318, 2012.
38. Berikol, G.B., Yildiz, O., and Özcan, İ.T., Diagnosis of acute coronary syndrome with a support vector machine. *J. Med. Syst.* 40:84, 2016.
39. Cortes, C., and Vapnik, V., Support-vector networks. *Mach. Learn.* 20(3):273, 1995.
40. Leartveravat, S., Transcutaneous bilirubin measurement in full term neonate by digital camera. *Medical Journal of Srisaket Surin Buriram Hospitals.* 24(1):105–118, 2009.
41. Nagar, G., Vandermeer, B., Campbell, S., and Kumar, M., Reliability of transcutaneous bilirubin devices in preterm infants: a systematic review. *Pediatrics*. 132(5):871–881, 2013.